Cell Stem Cell
Article

Telomeres Acquire Embryonic Stem Cell Characteristics in Induced Pluripotent Stem Cells

Rosa M. Marion,[1,4] Katerina Strati,[1,4] Han Li,[2] Agueda Tejera,[1] Stefan Schoeftner,[1] Sagrario Ortega,[3] Manuel Serrano,[2] and Maria A. Blasco[1,*]
[1]Telomeres and Telomerase Group, Molecular Oncology Program
[2]Tumor Suppression Group, Molecular Oncology Program
[3]Transgenic Mice Unit, Biotechnology Program
Spanish National Cancer Centre (CNIO), Melchor Fernández Almagro 3, Madrid E-28029, Spain
[4]These authors contributed equally to this work
*Correspondence: mblasco@cnio.es
DOI 10.1016/j.stem.2008.12.010

SUMMARY

Telomere shortening is associated with organismal aging. iPS cells have been recently derived from old patients; however, it is not known whether telomere chromatin acquires the same characteristics as in ES cells. We show here that telomeres are elongated in iPS cells compared to the parental differentiated cells both when using four (Oct3/4, Sox2, Klf4, cMyc) or three (Oct3/4, Sox2, Klf4) reprogramming factors and both from young and aged individuals. We demonstrate genetically that, during reprogramming, telomere elongation is usually mediated by telomerase and that iPS telomeres acquire the epigenetic marks of ES cells, including a low density of trimethylated histones H3K9 and H4K20 and increased abundance of telomere transcripts. Finally, reprogramming efficiency of cells derived from increasing generations of telomerase-deficient mice shows a dramatic decrease in iPS cell efficiency, a defect that is restored by telomerase reintroduction. Together, these results highlight the importance of telomere biology for iPS cell generation and functionality.

INTRODUCTION

Induced pluripotent stem (iPS) cells derived from differentiated somatic cells represent a new source of stem cells for customized transplantation therapies (Takahashi and Yamanaka, 2006; Wernig et al., 2007; Takahashi et al., 2007; Stadtfeld et al., 2008; Maherali et al., 2007; Okita et al., 2007; Nakagawa et al., 2008; Aoi et al., 2008). In particular, a combination of a few factors related to stem cell pluripotency allowed reprogramming of differentiated mouse and human cells into iPS cells (Takahashi and Yamanaka, 2006; Wernig et al., 2007; Takahashi et al., 2007; Stadtfeld et al., 2008; Maherali et al., 2007; Okita et al., 2007; Nakagawa et al., 2008; Aoi et al., 2008). These factors include Oct3/4 (also called Pou5f1), Sox2, Klf4, and cMyc; the latter was found dispensable for iPS cell generation (Nakagawa et al., 2008). Although full characterization of iPS cells is still in progress, iPS cells seem to have the same properties as embryonic stem (ES) cells and share with them a similar global gene expression pattern, including a correct genome-wide epigenetic reprogramming (Takahashi and Yamanaka, 2006; Wernig et al., 2007; Maherali et al., 2007; Mikkelsen et al., 2008). Furthermore, iPS cells contribute to mouse embryonic development and to the mouse germline (Takahashi and Yamanaka, 2006; Wernig et al., 2007; Takahashi et al., 2007; Stadtfeld et al., 2008; Maherali et al., 2007; Okita et al., 2007; Nakagawa et al., 2008; Aoi et al., 2008), supporting the notion that they are pluripotent and indistinguishable from ES cells. In the case of regenerative transplantation therapies, these findings open the possibility of using iPS cells derived from patients as a way to bypass the technical difficulties, as well as ethical controversies, associated with the alternative method of nuclear transfer to human oocytes, in vitro generation of preimplantation embryos, and obtention of ES cells.

Telomeres have been shown to shorten associated to increasing age (Harley et al., 1990) and contribute to organismal aging by limiting the proliferative capacity of adult stem cells (Blasco, 2007a; Flores et al., 2005, 2006a). Although telomerase activity has been found upregulated in both human and mouse iPS cells (Takahashi et al., 2007; Stadtfeld et al., 2008) and iPS cells have been recently derived from very old patients (Dimos et al., 2008), it is not known whether telomeres are re-elongated and whether telomeric chromatin acquires the same characteristics as in ES cells. For example, telomerase is reactivated in human cancers; however, the telomeres of most cancer cells are shorter than those of normal tissues (de Lange et al., 1990; Meeker et al., 2004).

Telomeres are ribonucleoprotein heterochromatic structures at the ends of chromosomes that protect them from degradation and recombination activities (Blackburn, 2001). Telomeres consist of tandem repeats of the TTAGGG sequence bound to a 6 protein complex known as shelterin (Blackburn, 2001; de Lange, 2005). Telomere length is influenced by changes in the activity of telomerase, the reverse transcriptase that elongates telomeres (Greider and Blackburn, 1985), as well as by the so-called alternative lengthening of telomeres or ALT pathway, which relays in homologous recombination between telomeric sequences (Dunham et al., 2000). In turn, these telomere-elongating mechanisms are regulated by the epigenetic status of telomeric chromatin (Blasco, 2007b). In particular, both telomeric

and subtelomeric repeats are enriched in histone methylation marks characteristic of repressed heterochromatic domains such as trimethylation of H3K9 and H4K20, and they show binding of the heterochromatin protein 1 (HP1) (García-Cao et al., 2004; Gonzalo et al., 2006; Benetti et al., 2007). In addition, the DNA of subtelomeric repeats is heavily methylated (Gonzalo et al., 2006). Loss of these epigenetic marks results in derepression of telomere recombination and telomere elongation (García-Cao et al., 2004; Gonzalo et al., 2006; Benetti et al., 2007). Furthermore, telomeres are transcribed, and the resulting UUAGGG-rich RNAs (TelRNAs or TERRAs) remain bound to the telomeric chromatin, where they are proposed to regulate telomere length (Azzalin et al., 2007; Schoeftner and Blasco, 2008). Telomerase is expressed during embryonic development and in the stem cell compartment of several adult tissues (Blasco, 2007a; Flores et al., 2005; 2006a; Liu et al., 2007); however, telomerase levels in these tissues are not sufficient to prevent progressive telomere shortening with age both in humans and mice (Harley et al., 1990; Flores et al., 2008). Reduced telomerase activity due to mutations in telomerase components in the human diseases dyskeratosis congenita, aplastic anemia, and idiopathic pulmonary fibrosis (Mitchell et al., 1999; Yamaguchi et al., 2005; Tsakiri et al., 2007; Armanios et al., 2007) further accelerates telomere shortening and leads to premature loss of tissue regeneration, suggesting that telomerase levels in the adult organism are rate limiting and influence organ homeostasis. Further evidence for a role of telomerase and telomere length in organ homeostasis comes from the study of telomerase-deficient mice (*Terc*$^{-/-}$ mice), which show premature aging and a decreased proliferative potential of adult stem cell populations (Blasco et al., 1997; Lee et al., 1998; Herrera et al., 1999; Samper et al., 2002; Ferrón et al., 2004). Therefore, the functionality of iPS cells could be limited in elderly patients or in patients with a limited telomere reserve, and the resulting iPS cells could inherit telomeric defects, including suboptimal telomere length. In this regard, previous studies with cloned animals by means of somatic cell nuclear transfer into enucleated oocytes have rendered contradictory results regarding whether telomeres are elongated or not during nuclear reprogramming (Shiels et al., 1999; Vogel, 2000; Lanza et al., 2000). On one hand, the cloned sheep Dolly showed abnormally short telomeres, something that was attributed to the adult origin of the donor nucleus (Shiels et al., 1999), whereas cloning of cattle or mice for six generations had no notable effect on telomere length (Lanza et al., 2000; Wakayama et al., 2000).

Finally, it is known that, soon after fertilization but previous to the formation of the blastocyst, telomeres are elongated by a telomerase-independent recombination-based mechanism (Liu et al., 2007). This opens several scenarios for the reprogramming of telomeric chromatin, including dispensability of telomerase for telomere elongation, cooperation between telomerase-based and recombination-based mechanisms, and, finally, complete dependence on telomerase for telomere elongation during reprogramming.

Here, we show that both telomere length and telomere heterochromatic marks acquire ES cell features during iPS cell generation. Importantly, we show here that telomeres are also efficiently elongated in iPS cells derived from old animals, demonstrating that telomeres can be efficiently rejuvenated during nuclear reprogramming. Interestingly, we show that telomerase activity is the primary mechanism to mediate telomere re-elongation during reprogramming and that a minimum telomere length is necessary for iPS cell generation. In particular, cells derived from telomerase-deficient mice fail to properly elongate telomeres during reprogramming, and telomeres continue to shorten during iPS cell generation. Furthermore, an increasing number of generations of telomerase-deficient mice with progressive shorter telomeres show a dramatic impairment in iPS cell generation. These findings highlight the importance of telomere biology for the generation and proper functionality of iPS cells.

RESULTS

cMyc Is Dispensable for Telomerase Activation in Mouse iPS Cells

Telomerase activity has been previously shown to increase during iPS cell generation using a combination of four reprogramming factors (Takahashi et al., 2007; Maherali et al., 2007; Zhao and Daley, 2008), namely Oct3/4, Sox2, Klf4, and cMyc, the latter being a transcriptional activator of telomerase in the mouse (Wu et al., 1999; Flores et al., 2006b). Here, we address the putative role of cMyc in telomerase activation during mouse iPS cell generation by comparing telomerase activity levels in mouse iPS cells generated with four factors (Oct3/4, Sox2, Klf4, and cMyc; referred to here as 4F iPS cells) with those of iPS cells generated with three factors in the absence of cMyc (Oct3/4, Sox2, and Klf4; referred to here as 3F iPS cells) (Nakagawa et al., 2008; Wernig et al., 2008). To this end, 3F and 4F mouse iPS cells were generated from mouse embryonic fibroblasts (MEF) as previously described (Takahashi and Yamanaka, 2006; Nakagawa et al., 2008) (Experimental Procedures). The resulting iPS cells showed expression of the endogenous factors and a similar morphology to ES cells; stained positive for alkaline phosphatase; maintained the ES cell morphology upon expansion; and expressed the stemness marker Nanog (Figures S1A–S1E available online). Importantly, both 3F and 4F iPS cells were able to contribute to mouse embryonic development as indicated by important mouse chimerism when microinjected into C57BL6-Tyr^{c} (albino) blastocysts (Figure S1F and Table 1) or when aggregated with CD1 (albino) morulae (Table 1). In both cases, around 30% of the pups born were chimeras as judged by the coat color, with iPS contribution to the coat in a range of 60%–100% in the case of microinjected blastocysts and 5%–50% in the case of aggregation to morulae (Figure S1F and Table 1). Furthermore, both 3F and 4F iPS cells showed germline transmission (Table 1). These results indicate that the 3F and 4F wild-type iPS cells generated for this study are pluripotent and are able to contribute to the mouse germline. In agreement with this, iPS cells showed a normal chromosomal ploidy (Figures S2A and S2B).

Telomerase activity was increased ~9-fold in 4F iPS cell clones, compared to the parental MEF, reaching slightly higher levels than those of control ES cells in the same genetic background (Figures S3A and S3B) (Takahashi et al., 2007; Maherali et al., 2007; Zhao and Daley, 2008). A similar 8-fold increase in telomerase activity was detected in the 3F iPS cells generated in the absence of the cMyc reprogramming factor (Figures S3A

Table 1. Generation of Chimeras and Germline Transmission with C57BL/6 WT iPS Clones Reprogrammed with Three (3F) or Four (4F) Factors

Microinjection in B6-*tyr*$^{C-2J}$ Blastocysts					
iPS clone	Blastocysts Injected	Cells Injected	Blastocysts Transferred	Pups Born	Chimeras Sex (% Pigmentation)
iPS (3F)-7 *wt*	52	5–8	52	5	1M (100%)[a]
iPS (3F)-9 *wt*	43	5–8	43	4	1F (60%)
iPS (4F)-4 *wt*	58	5–6	58	8	2M (80%)[a] 1F (100%)
Aggregation with CD1 Morulae					
iPS Clone	Morulae Aggregated	Cells Aggregated	Pups Born	Chimeras Sex (% Pigmentation)	
iPS (4F)-3 *wt*	171	4–8	15	1M (30%) 1M (5%) 1F (50%) 2F (30%)	
3F and 4F WT iPS contribution to the germline					
Chimeras × B6-*tyr*$^{C-2J}$ Females					
iPS Clone	Chimera Sex (% Pigmentation)	Black/White Pups			
iPS (4F)-4 *wt*	M (80%)	5/14			
	M (80%)	8/10			
iPS (3F)-7 *wt*	M (100%)	11/0			

[a] Germline chimeras.

and S3B). These results indicate that cMyc is not essential to up-regulate telomerase activity during iPS cell generation. In this regard, MEF have high levels of cMyc and may not need additional cMyc activity to re-express telomerase during iPS cell generation (Takahashi et al., 2007).

Next, we addressed whether telomerase activation per se was necessary for efficient iPS cell formation by using cells derived from first generation (G1) telomerase-deficient *Terc*$^{-/-}$ mice in a C57BL6 genetic background (Herrera et al., 1999). We were able to generate iPS cells from G1 telomerase-deficient MEF to a similar efficiency to wild-type MEF (Figures 2A and 2B), indicating that activation of telomerase per se is not necessary for iPS cell generation, at least in the presence of a sufficient telomere reserve, such as in the case of G1 *Terc*$^{-/-}$ mice (Herrera et al., 1999). As expected, telomerase activity was negative both in parental MEF and in iPS derived from G1 telomerase-deficient mice (Figures S3A and S3B). Interestingly, in spite of a normal efficiency of G1 *Terc*$^{-/-}$ iPS cell generation compared to wild-type controls, we failed to obtain any viable chimeric mice from these cells. In particular, from a total of 11 pups born, only one showed a high level of iPS contribution as judged by eye pigmentation; however, these mice did not survive, in contrast to a 100% survival in the case of chimeras derived from wild-type iPS cells (Table 2). These results indicate that telomerase activity is not limiting for in vitro iPS cell proliferation when telomeres are sufficiently long, such as in the case of G1 telomerase-deficient iPS cells. However, these cells are severely impaired in their ability to generate viable mice compared to wild-type telomerase-proficient 3F and 4F iPS cells, most likely due to increased chromosomal instability (see Figure 2).

Telomere Elongation by Telomerase in iPS Cells

Next, we addressed whether telomeres were elongated during the reprogramming of 3F and 4F iPS cells (all at passage 8) compared to control ES cells by measuring telomere length in individual clones of these cells using two independent techniques, Southern telomere restriction analysis (TRF) and quantitative telomere FISH (Q-FISH) on metaphase spreads (Experimental Procedures). Telomeres were elongated in wild-type 4F iPS cells compared to the corresponding parental wild-type MEF, both as determined by TRF (Figure 1A) and Q-FISH analyses (Figures 1B–1E). Telomeres were also elongated in 3F iPS cells but did not reach the length of 4F iPS cells (Figures 1A–1E), although both had similar levels of telomerase activity (Figures S3A and S3B). Of notice, whereas the freshly emerged colonies of wild-type 3F and 4F iPS cells have

Table 2. Generation of Chimeras with C57BL/6 G1–G3 *Terc*$^{-/-}$ Mutant iPS Clones

Microinjection in B6-*tyr*$^{C-2J}$ Blastocysts						
iPS Clone	MEFs Genotype	Blastocysts Injected	Cells Injected	Blastocysts Transferred	Pups Born	Chimeras
iPS (3F) 718-7.1	G1 *Terc*$^{-/-}$	36	5–7	36	10 + 1 dead	1 dead[a]
iPS (3F) 710-8.1	G2 *Terc*$^{-/-}$	40	5–7	40	11	0
Aggregation with CD1 Morulae						
iPS Clone	MEFs Genotype	Morulae Aggregated	Cells Aggregated	Embryos Transferred	Pups Born	Chimeras Sex (% Pigmentation
iPS (3F) 710-8.4	G2 *Terc*$^{-/-}$	96	4–6	96	15 + 1 dead	0[b]
iPS (3F) 62T1-1	G3 *Terc*$^{-/+*}$	153	4–12	153	15 + 4 dead	1M (100%) 1M (70%) 1F (30%) + 3 dead[a]

[a] The dead pups had pigmented eyes.
[b] By eye pigmentation.

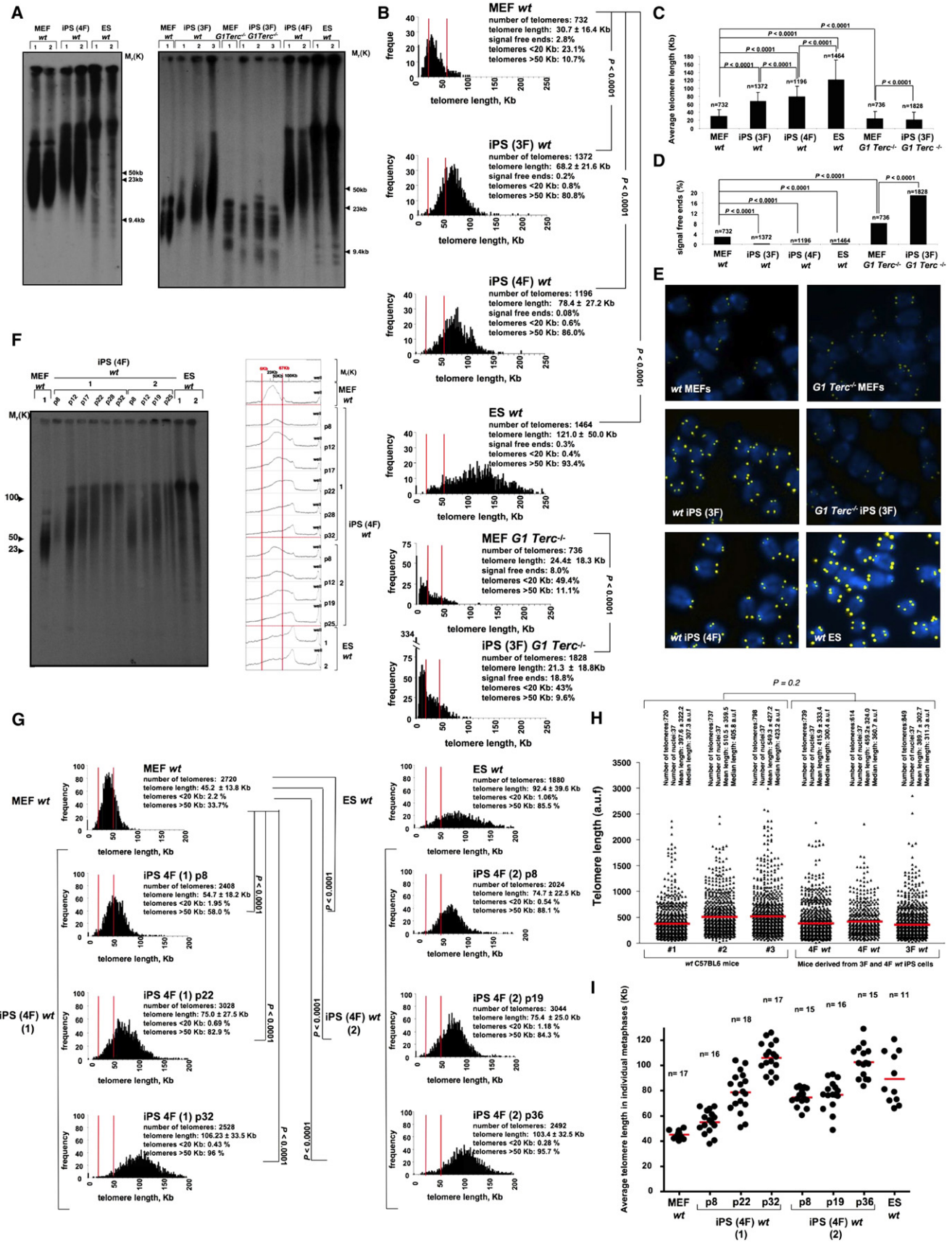
A
MEF wt
iPS (4F) wt
ES wt
MEF wt
iPS (3F) wt
MEF G1Terc-/-
iPS (3F) G1Terc-/-
iPS (4F) wt
ES wt
Mr(K)
50kb
23kb
9.4kb
B
MEF wt
number of telomeres: 732
telomere length: 30.7 ± 16.4 Kb
signal free ends: 2.8%
telomeres <20 Kb: 23.1%
telomeres >50 Kb: 10.7%
iPS (3F) wt
number of telomeres: 1372
telomere length: 68.2 ± 21.6 Kb
signal free ends: 0.2%
telomeres <20 Kb: 0.8%
telomeres >50 Kb: 80.8%
iPS (4F) wt
number of telomeres: 1196
telomere length: 78.4 ± 27.2 Kb
signal free ends: 0.08%
telomeres <20 Kb: 0.6%
telomeres >50 Kb: 86.0%
ES wt
number of telomeres: 1464
telomere length: 121.0 ± 50.0 Kb
signal free ends: 0.3%
telomeres <20 Kb: 0.4%
telomeres >50 Kb: 93.4%
MEF G1 Terc-/-
number of telomeres: 736
telomere length: 24.4± 18.3 Kb
signal free ends: 8.0%
telomeres <20 Kb: 49.4%
telomeres >50 Kb: 11.1%
iPS (3F) G1 Terc-/-
number of telomeres: 1828
telomere length: 21.3 ± 18.8Kb
signal free ends: 18.8%
telomeres <20 Kb: 43%
telomeres >50 Kb: 9.6%
telomere length, Kb
frequency
P < 0.0001
C
Average telomere length (Kb)
n=732
n=1372
n=1196
n=1464
n=736
n=1828
MEF wt
iPS (3F) wt
iPS (4F) wt
ES wt
MEF G1 Terc-/-
iPS (3F) G1 Terc -/-
D
signal free ends (%)
E
wt MEFs
G1 Terc-/- MEFs
wt iPS (3F)
G1 Terc-/- iPS (3F)
wt iPS (4F)
wt ES
F
iPS (4F) wt
MEF wt
ES wt
Mr(K)
100
50
23
MEF wt
iPS (4F) wt
ES wt
G
MEF wt
number of telomeres: 2720
telomere length: 45.2 ± 13.8 Kb
telomeres <20 Kb: 2.2 %
telomeres >50 Kb: 33.7%
iPS 4F (1) p8
number of telomeres: 2408
telomere length: 54.7 ± 18.2 Kb
telomeres <20 Kb: 1.95 %
telomeres >50 Kb: 58.0 %
iPS 4F (1) p22
number of telomeres: 3028
telomere length: 75.0 ± 27.5 Kb
telomeres <20 Kb: 0.69 %
telomeres >50 Kb: 82.9 %
iPS 4F (1) p32
number of telomeres: 2528
telomere length: 106.23 ± 33.5 Kb
telomeres <20 Kb: 0.43 %
telomeres >50 Kb: 96 %
iPS (4F) wt (1)
ES wt
number of telomeres: 1880
telomere length: 92.4 ± 39.6 Kb
telomeres <20 Kb: 1.06%
telomeres >50 Kb: 85.5 %
iPS 4F (2) p8
number of telomeres: 2024
telomere length: 74.7 ± 22.5 Kb
telomeres <20 Kb: 0.54 %
telomeres >50 Kb: 88.1 %
iPS 4F (2) p19
number of telomeres: 3044
telomere length: 75.4 ± 25.0 Kb
telomeres <20 Kb: 1.18 %
telomeres >50 Kb: 84.3 %
iPS 4F (2) p36
number of telomeres: 2492
telomere length: 103.4 ± 32.5 Kb
telomeres <20 Kb: 0.28 %
telomeres >50 Kb: 95.7 %
iPS (4F) wt (2)
P < 0.0001
telomere length, Kb
frequency
H
P = 0.2
Telomere length (a.u.f)
#1
#2
#3
4F wt
4F wt
3F wt
wt C57BL6 mice
Mice derived from 3F and 4F wt iPS cells
I
Average telomere length in individual metaphases (Kb)
n= 17
n= 16
n= 18
n= 17
n= 15
n= 16
n= 15
n= 11
MEF wt
p8
p22
p32
p8
p19
p36
ES wt
iPS (4F) wt (1)
iPS (4F) wt (2)

telomeres that are not as long as the telomeres of control ES cells in the same genetic background, upon a limited number of passages in vitro, the iPS telomeres eventually reached full ES telomere length (Figures 1F and 1G), in accordance with previous findings showing that telomerase needs a number of cell divisions in vivo in order to restore a normal average telomere length (Siegl-Cachedenier et al., 2007). Furthermore, an increasing number of passages of wild-type iPS cells retained a normal telomere-capping function as indicated by normal ploidy and a low frequency of end-to-end fusions and of signal-free ends (Figures S4A–S4C), in agreement with the fact that they produced mice with a high degree of chimerism and contributed to the mouse germline (Figure S1 and Table 1). Furthermore, telomere length in the tail skin of iPS cell-derived mice was similar to that of age-matched, sex-matched wild-type C57BL6 controls (Figure 1H), indicating normal telomere dynamics in these mice. Finally, by analyzing telomere length of single MEF and iPS cells at different passages, we observed the appearance of iPS cells with progressively longer telomeres compared to MEF (Figure 1I). Furthermore, the fact that, at their time of isolation (passage 8), iPS cell clones had telomeres only moderately longer than MEF, which are further elongated with increasing passages, suggests that most telomere elongation occurs postreprogramming.

Next, we addressed whether telomere elongation in iPS cells was mediated by telomerase activity and/or by telomere-lengthening mechanisms alternative to telomerase, which are based on recombination between telomeric sequences (Dunham et al., 2000) and are described to mediate telomere elongation in early cleavage embryos (Liu et al., 2007). To this end, we measured telomere length in iPS cells (3F) derived from G1 *Terc*$^{-/-}$ MEF. As shown both by TRF and Q-FISH techniques, telomeres were further shortened in iPS cells derived from G1 *Terc*$^{-/-}$ MEF compared to the parental wild-type MEF (Figures 1A–1E), indicating that telomerase is the primary activity responsible for telomere elongation in telomerase-proficient iPS cells. Signal-free ends (chromosome ends with undetectable telomere signals or critically short telomeres) were decreased in telomerase-proficient 3F and 4F iPS cells compared to parental MEF, reaching similar levels to those of control ES cells (Figure 1D), in agreement with re-elongation of short telomeres by telomerase during iPS cell generation. In contrast, this was not observed in *Terc*$^{-/-}$ iPS cells, which showed a further increase in signal-free ends compared to the parental G1 *Terc*$^{-/-}$ MEF (Figure 1D). Finally, the fact that G1 *Terc*$^{-/-}$ iPS cell telomeres shortened compared to the parental MEF argues against telomere recombination mechanisms operating to elongate telomeres during iPS cell nuclear reprogramming, at least in early-generation G1 *Terc*$^{-/-}$ cells. These results are in agreement with telomere recombination operating from zygote to blastocyst and switching to telomerase at the blastocyst stage (Liu et al., 2007).

Impaired iPS Cell Generation from Late-Generation *Terc*$^{-/-}$ MEF with Critically Short Telomeres

To address whether telomere shortening in the absence of telomerase activity could eventually limit iPS cell generation, we compared the frequencies of iPS cell generation from G1, G2, and G3 telomerase-deficient MEF. Again, whereas G1 *Terc*$^{-/-}$ MEF yielded a normal efficiency of iPS cell generation compared to wild-type MEF, we detected a dramatic decrease in the efficiency of iPS cell generation in G2 and G3 *Terc*$^{-/-}$ MEF (Figures 2A and 2B), indicating that telomere shortening represents a potent barrier against iPS cell generation in telomerase-deficient cells. In addition, similarly to that previously observed for G1 *Terc*$^{-/-}$ iPS cells, G2 *Terc*$^{-/-}$ iPS cells failed to generate viable chimeric mice (Table 2). Importantly, the decreased iPS cell generation was coincidental with shorter telomeres both as determined by TRF (Figure 2C) and Q-FISH analysis (Figures 2D and 2E) and by an increase in signal-free ends and chromosome end-to-end fusions in the parental G1–G3 *Terc*$^{-/-}$ MEF compared to wild-type MEF, which was further aggravated in the corresponding G1–G3 *Terc*$^{-/-}$ iPS clones (Figures 2F and 2G). Interestingly, both when using TRF and Q-FISH analysis, we noticed that average telomere length was not further shortened in G2 and G3 *Terc*$^{-/-}$ iPS cell clones compared to the parental G2-G3 MEF (Figures 2C–2E; see asterisk in Figure 2C), suggesting the activation of telomerase-independent telomere elongation mechanisms in some G2-G3 *Terc*$^{-/-}$ iPS cell clones (Figures 2A and 2B). Of notice, telomerase-independent telomere elongation mechanisms typically lead to heterogeneous telomere length distributions, with the presence of

Figure 1. Telomerase-Dependent Telomere Elongation in Mouse iPS Cells

(A) TRF analysis. Two representative TRF gels are shown. Note the longer telomeres in wild-type 3F and 4F iPS cells compared to the parental MEF. In contrast, G1 *Terc*$^{-/-}$ iPS cells show shorter telomeres compared to parental MEF. Numbers refer to two to three independent cell cultures per cell type. MEF passage number = 2; iPS passage number = 8.

(B) Telomere length distribution as determined by Q-FISH on metaphases. Two to three cell cultures per cell type were used for the analysis. MEF passage number = 2; iPS passage number = 8. A Wilcoxon-Mann-Whitney rank sum test was used to calculate statistical significance of differences in telomere length.

(C) Quantification of average telomere length in kilobases. n, number of telomeres. MEF passage number = 2; iPS passage number = 8. Error bars, SD.

(D) Quantification of the percentage of signal-free ends. MEF passage number = 2; iPS passage number = 8. Error bars, SD. Statistical comparisons using chi-square test are shown.

(E) Representative images of metaphasic chromosomes after telomere Q-FISH. Yellow, telomeres; blue, DAPI. MEF passage number = 2; iPS passage number = 8.

(F) TRF analysis of two independent 4F iPS cell clones at the indicated passages. Right panel shows the signal distribution in each TRF lane.

(G) Telomere length distributions at different passages as determined by Q-FISH on metaphases. Telomere length of iPS cells increases with the passages, reaching that of control ES cells. A Wilcoxon-Mann-Whitney rank sum test was used for statistical calculations.

(H) Telomere length by Q-FISH on tail skins. Samples were obtained from three iPS cell-derived mice (two from 4F-reprogrammed iPS cells and one from 3F reprogrammed iPS cells) and three age-matched, sex-matched wild-type *C57BL6* mice. The number of telomeres and nuclei analyzed are indicated. Telomere length is shown in arbitrary fluorescence units (a.u.f.). Statistical analysis was performed using the Student's t test.

(I) Average telomere length in kilobases of individual MEF and iPS cells as determined by Q-FISH. "1" and "2" indicate independent iPS cell clones. Each dot represents the telomere length of a single metaphase. n, number of metaphases. p, passage number.

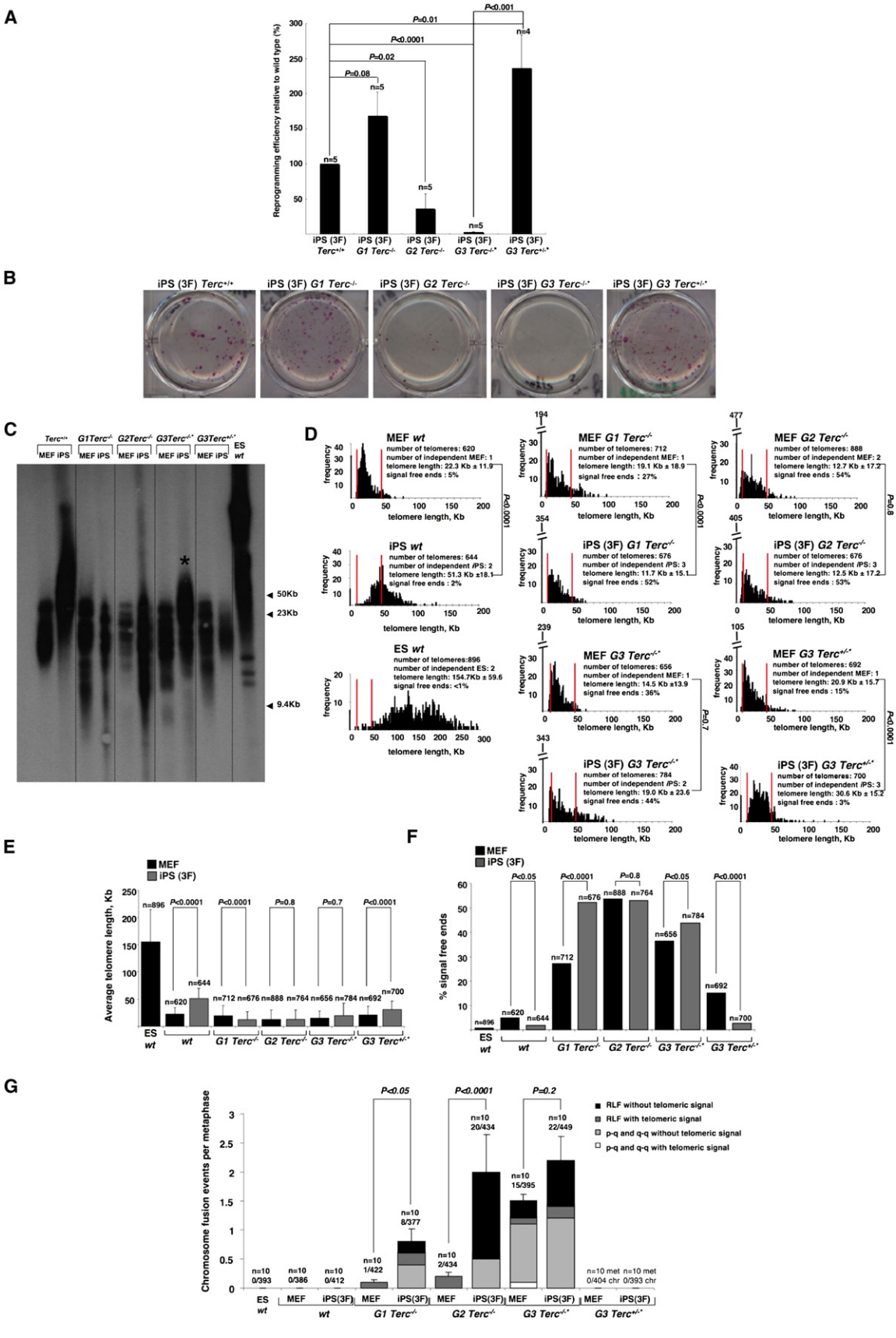
A
Reprogramming efficiency relative to wild type (%)
P=0.01
P<0.001
P<0.0001
P=0.02
P=0.08
n=5
n=4
iPS (3F) Terc+/+
iPS (3F) G1 Terc-/-
iPS (3F) G2 Terc-/-
iPS (3F) G3 Terc-/-*
iPS (3F) G3 Terc+/-*
B
iPS (3F) Terc+/+
iPS (3F) G1 Terc-/-
iPS (3F) G2 Terc-/-
iPS (3F) G3 Terc-/-*
iPS (3F) G3 Terc+/-*
C
MEF iPS
ES wt
50Kb
23Kb
9.4Kb
D
MEF wt
iPS wt
ES wt
MEF G1 Terc-/-
iPS (3F) G1 Terc-/-
MEF G2 Terc-/-
iPS (3F) G2 Terc-/-
MEF G3 Terc-/-*
iPS (3F) G3 Terc-/-*
MEF G3 Terc+/-*
iPS (3F) G3 Terc+/-*
frequency
telomere length, Kb
E
MEF
iPS (3F)
Average telomere length, Kb
P<0.0001
P=0.8
P=0.7
n=896
n=620
n=644
n=712
n=676
n=888
n=764
n=656
n=784
n=692
n=700
ES wt
wt
G1 Terc-/-
G2 Terc-/-
G3 Terc-/-*
G3 Terc+/-*
F
% signal free ends
P<0.05
P=0.8
n=676
n=888
n=764
n=656
n=784
n=712
n=692
G
Chromosome fusion events per metaphase
P<0.05
P<0.0001
P=0.2
RLF without telomeric signal
RLF with telomeric signal
p-q and q-q without telomeric signal
p-q and q-q with telomeric signal
n=10 0/393
n=10 0/386
n=10 0/412
n=10 1/422
n=10 8/377
n=10 2/434
n=10 20/434
n=10 15/395
n=10 22/449
n=10 met 0/404 chr
n=10 met 0/393 chr
MEF
iPS(3F)

very short and long telomeres (see G3 *Terc*$^{-/-}$ iPS cell telomeres in Figures 2C and 2D).

Elongation of short telomeres by telomerase in *Terc*-reconstituted mice is sufficient to rescue telomere dysfunction, as well as degenerative pathologies and decreased life span associated with telomere dysfunction in *Terc*$^{-/-}$ mice (Hemann et al., 2001; Samper et al., 2001; Siegl-Cachedenier et al., 2007). Here, we addressed whether telomerase reintroduction into G3 *Terc*$^{-/-}$ MEF by means of mouse crosses between *Terc*$^{+/-}$ mice and G2 *Terc*$^{-/-}$ mice was sufficient to rescue critically short telomeres and iPS cell generation in MEF derived from the G3 *Terc*$^{-/+*}$ offspring compared to the G3 *Terc*$^{-/-*}$ littermates. As shown in Figures 2A and 2B, iPS cell efficiency was fully restored to wild-type levels in G3 *Terc*$^{-/+*}$ cells compared to G3 *Terc*$^{-/-*}$ cells, both of which inherited short telomeres from the G2 *Terc*$^{-/-}$ parent. This rescue of iPS cell generation when using G3 *Terc*$^{-/+*}$ MEF was concomitant with the disappearance of critically short telomeres (signal-free ends) and with rescue of chromosome end-to-end fusions in the G3 *Terc*$^{-/+*}$ iPS cells compared to iPS derived from G3 *Terc*$^{-/-*}$ littermates (Figures 2F and 2G). Of interest, average telomere length in G3 *Terc*$^{-/+*}$ iPS cells was not fully restored to that of wild-type iPS cells (Figures 2C–2E), in agreement with previous reports showing that telomerase preferentially elongates the very short telomeres (Hemann et al., 2001; Samper et al., 2001) and that average telomere length is only recovered with time (Siegl-Cachedenier et al., 2007). These results indicate that presence of critically short telomeres, rather than average telomere length, is the key molecular event restricting iPS cell generation in the absence of telomerase enzymatic activity. In accordance with this finding, we were able to derive viable chimeric mice from G3 *Terc*$^{-/+*}$ iPS cells in contrast to G1–G3 *Terc*$^{-/-}$ iPS cells (Table 2).

Telomeric Heterochromatin in iPS Cells Acquires ES Cell Features

Epigenetic marks, such as DNA methylation of specific loci, are properly reprogrammed during iPS cell generation, reaching a pattern of DNA methylation similar to that shown by ES cells (Wernig et al., 2007). DNA methylation at pericentric repeats does not seem to undergo reprogramming for the trivial reason that it remains unaltered in ES cells, iPS cells, and differentiated cells (Wernig et al., 2007). Using 4F iPS, here we extend these observations to interspersed repeats (SINE repeats) and to subtelomeric repeats, which are also fully methylated in these three cell types (Figures 3A–3C). Together, these results suggest that DNA methylation of repeated regions in the genome such as pericentric repeats, SINE elements, and subtelomeric repeats does not significantly vary during nuclear reprogramming. In contrast, we observed a decrease in the density of H3K9m3 and H4K20m3 histone heterochromatic marks at the telomeres of iPS cells (passage 8) and ES cells compared to differentiated MEFs (Figure 4A). A similar decrease in these marks was also observed at pericentric repeats (Figure 4B). Importantly, this decrease in heterochromatic marks cannot be attributed to differences in the input of telomeric or pericentric DNA or in nucleosome density at these regions, as ChIP values were corrected both by telomere and centromere inputs, respectively, as well as by H3 and H4 abundance at these domains (Figures 4A and 4B). Of notice, we did not detect significant changes in the density of the TRF1 shelterin protein at telomeres between iPS cells, ES cells, and MEF (Figure 4A). As control, TRF1 was not detected at pericentric chromatin (Figure 4B).

We have previously described that heterochromatic marks at telomeres repress homologous recombination events between telomeric repeats (Gonzalo et al., 2006; Benetti et al., 2007). Next, we determined telomere recombination frequencies in ES cells, iPS cells, and parental MEF by using chromosome orientation-FISH (CO-FISH) (Experimental Procedures), which measures frequency of chromatid exchanges between sister telomeres (T-SCEs). Interestingly, iPS cells (passage 8) showed higher telomere recombination frequencies than parental MEF, reaching similar values to those of ES cells (Figure S5). Together, these results suggest that telomere chromatin adopts a less-compacted conformation in ES cells compared to differentiated cells and that telomeric chromatin in iPS cells resembles that of control ES cells.

Increased Telomere Transcription in iPS Cells

Telomere chromatin is transcribed, generating long noncoding UUAGGG-rich transcripts (TelRNAs or TERRAs) that remain associated to the telomeric chromatin (Azzalin et al., 2007; Schoeftner and Blasco, 2008), where they have been proposed to act as negative regulators of telomere length (Schoeftner and Blasco, 2008). In particular, abundance of TelRNAs is positively correlated with telomere length, and these RNAs can efficiently inhibit telomerase activity in in vitro TRAP assays (Schoeftner and Blasco, 2008). In agreement with their longer telomeres, we find that TelRNAs are more abundant in ES cells

Figure 2. Impaired iPS Cell Generation from Late Generation *Terc*$^{-/-}$ MEF with Critically Short Telomeres

(A) Quantification of relative efficiency of iPS cell clone generation. Values are normalized to viral transduction efficiency (EGFP fluorescence). Efficiency of iPS cell generation is decreased in G2 and G3 *Terc*$^{-/-}$ MEF but is fully restored upon telomerase reintroduction into G3 *Terc*$^{-/-}$ MEF (G3 *Terc*$^{-/+*}$ cells). Error bars, SE. Statistical analysis was performed using a Student's t test. n, number of independent measurements.

(B) Representative images of alkaline phosphatase-positive iPS cell clones.

(C) Telomere length analysis by TRF. Note that a subset of the telomeres is elongated in G2 and G3 *Terc*$^{-/-}$ iPS cell clones compared to the parental G2-G3 MEF (asterisk). MEF passage number = 2; iPS passage number = 8.

(D) Telomere length as determined by Q-FISH on metaphase spreads. Statistical significance values are shown as assessed by the Wilcoxon-Mann-Whitney rank sum test. MEF passage number = 2; iPS passage number = 8.

(E) Quantification of average telomere length in kilobases. n, number of telomeres analyzed. MEF passage number = 2; iPS passage number = 8. Error bars, SD.

(F) Quantification of the percentage of signal-free ends. MEF passage number = 2; iPS passage number = 8. Note the disappearance of signal-free ends in the G3 *Terc*$^{-/+*}$ iPS compared to the parental G3 *Terc*$^{-/+*}$ MEF. n, number of telomeres. Statistical comparisons using the chi-square test are shown.

(G) Frequency of end-to-end chromosome fusions. n, number of metaphases. The total number of fusions out of the number of chromosomes analyzed is also indicated. MEF passage number = 2; iPS passage number = 8. Chi-square test was used for statistical analysis. Error bars, SE.

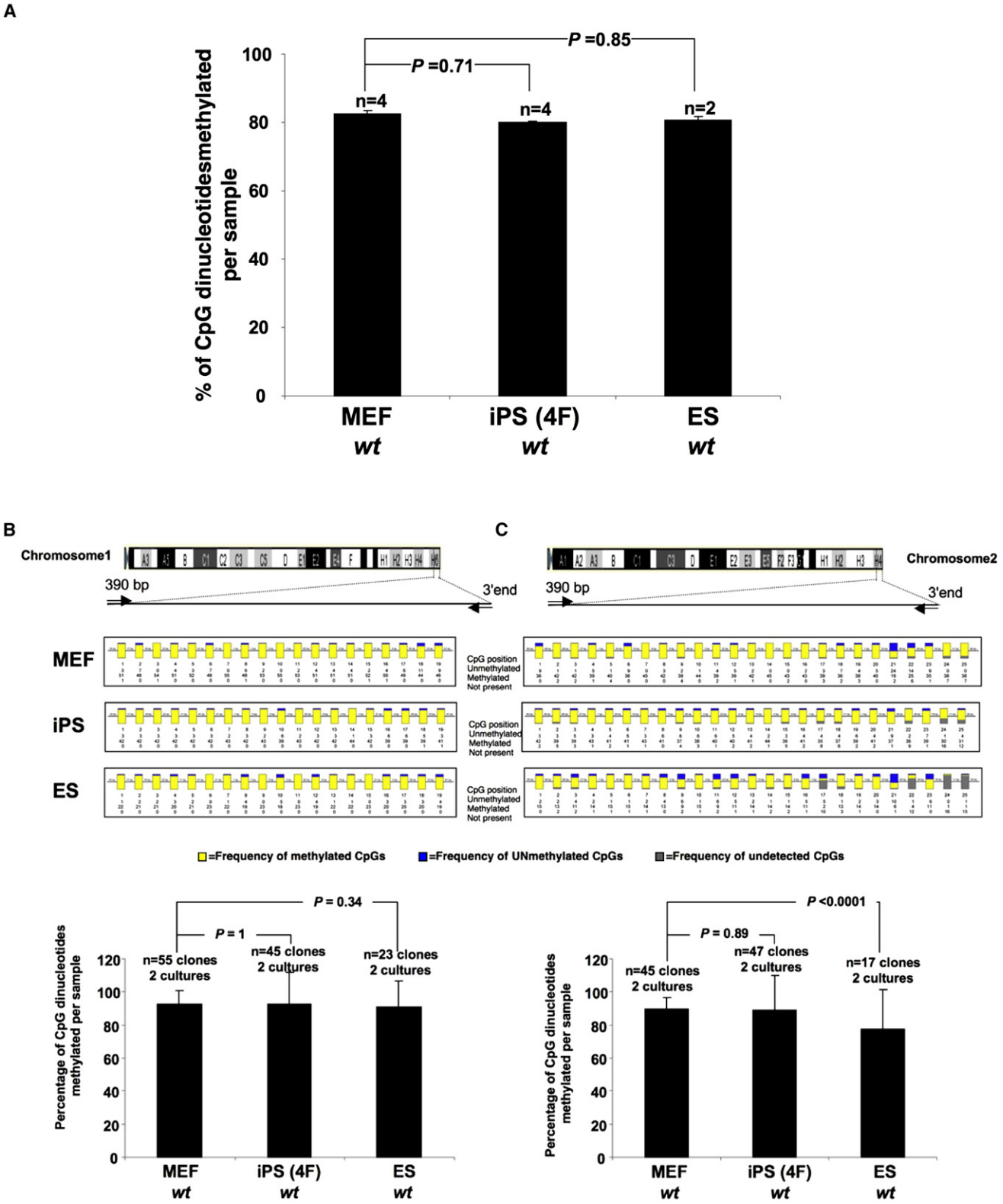

Figure 3. Global and Subtelomeric DNA Methylation in Mouse iPS Cells

(A) Fraction of methylated B1 SINE repeat elements. n, number of independent cell cultures. MEF passage number = 2; iPS passage number = 8. Statistical analysis was performed using a Student's t test. Error bars, SD.

than in differentiated MEF, whereas iPS (4F) (passage 8) show intermediate levels (Figures 4C and 4D), probably because additional rounds of cell division are needed to reach full telomere elongation by telomerase (Figures 1F and 1G). Intriguingly, production of centromeric transcripts was lower in ES cells compared to parental MEF, and a similar scenario was found for iPS cells (Figure 4C), pinpointing fundamental differences in the regulation of telomeric and centromeric transcription. In summary, these results indicate that iPS cell telomeres show higher transcriptional levels than differentiated cells, in agreement with their decreased density of histone heterochromatic marks (Figure 4A).

Telomere Elongation in iPS Cells Derived from Old Donors

Telomeres shorten with aging, and this telomere shortening is known to limit the proliferative capacity of stem cells. There is, therefore, an interesting question of whether telomere length of donor cells represents a potential barrier to the proper functionality of iPS cells and whether iPS cells derived from donors with a limited telomere reserve, such as elderly individuals or patients with diseases characterized by short telomeres, would inherit telomeric defects, including suboptimal telomere length. To address this question, we generated iPS cells from dermal skin fibroblast obtained from young (22 weeks old) and old (121 weeks old) mice (Figure 5). Dermal fibroblasts derived from old donors showed shorter telomeres than those of young dermal fibroblasts both when determined by TRF (Figure 5A) and by Q-FISH (Figures 5B and 5C), in agreement with telomere shortening with mouse aging (Flores et al., 2008). Importantly, telomeres of iPS cells from old donors were elongated similarly to those of iPS cells from young donors as indicated by TRF (Figure 5A) and Q-FISH (Figures 5B and 5C). The percentage of signal-free ends and the frequency of end-to-end fusions were also similarly low in iPS cells derived from young and old dermal fibroblasts (Figures 5D and 5E), suggesting normal telomere functionality in these cells.

DISCUSSION

We show here that mouse iPS cell telomeres adopt similar features to those of ES cell telomeres. In particular, telomere length was significantly increased in 3F and 4F iPS cells compared to parental differentiated cells, reaching intermediate levels to those of control ES cells in early passages but reaching telomere length comparable to control ES cells at later passages. We interpret that reprogramming changes the accessibility of telomerase to telomeres, allowing their progressive elongation until telomeres reach the length characteristic of ES cells.

A similar scenario is found for the generation of telomere RNAs, in agreement with the abundance of telomere transcripts being directly correlated with telomere length (Schoeftner and Blasco, 2008). In addition, telomere heterochromatin is remodeled in iPS cells to a similar conformation as that shown by ES cells' telomeric chromatin. In particular, both iPS and ES cells show a significant decrease in the density of histone heterochromatic marks (H3K9m3 and H4K30m3) at telomeric regions compared to differentiated MEF cells and present higher telomere recombination frequencies than parental MEF cells, suggesting a more relaxed chromatin conformation associated to pluripotent stem cells, in agreement with their higher transcriptional activity. These results go in line with the recent findings, suggesting a higher plasticity in the chromatin of pluripotent embryonic stem cells compared to differentiated cells (Meshorer et al., 2006).

Importantly, we show that donor cells with short telomeres obtained from old animals show telomere elongation and functional telomere capping during reprogramming into iPS cells, predicting full functionality and long-term regenerative potential of iPS derived from individuals with a limited telomere reserve, such as elderly individuals or patients suffering from diseases characterized by short telomeres (Blasco, 2005). However, these results also raise the potential problem of a less efficient reprogramming of iPS cells derived from patients with germline telomerase mutations, such as dyskeratosis congenita and some cases of aplastic anemia and idiopathic pulmonary fibrosis, as telomere elongation during iPS cell generation requires an active telomerase complex. This is supported by our findings showing that MEF derived from increasing generations of *Terc*-deficient mice have a decreased iPS cell efficiency from the second generation onward, which is concomitant with the presence of short telomeres and increased chromosomal aberrations. This parallels the decreased stem cell functionality of different adult stem cell compartments of telomerase-deficient mice, including neural stem cells, epidermal stem cells, and hematopoietic stem cells (Samper et al., 2002; Allsopp et al., 2003; Ferrón et al., 2004; Flores et al., 2005). Importantly, the fact that telomerase reintroduction and re-elongation of short telomeres are sufficient to restore a normal iPS cell generation and iPS cell functionality, as determined by generation of viable chimeras in late-generation telomerase-deficient MEF, pinpoints to telomerase reactivation as a putative therapeutic strategy to derive functional iPS cells from patients harboring telomerase mutations and a limited telomere reserve.

EXPERIMENTAL PROCEDURES

Generation of Mouse iPS Cells

Reprogramming of primary (passage 2–4) MEF derived either from wild-type or different generation (G1–G3) telomerase null *Terc*$^{-/-}$ embryos (MEFs of C57BL6 genetic background) or skin fibroblasts derived from young and old animals was performed essentially as described (Blelloch et al., 2007). Briefly, retroviral supernatants were produced in HEK293T cells (5 × 10^6 cells per 100 mm diameter dish) transfected with the ecotropic packaging plasmid pCL-Eco (4 μg) together with either one of the following retroviral constructs (4 μg): pMXs-cMyc, pMXs-Klf4, pMXs-Sox2, or pMXs-Oct3/4 (Addgene). Transfections were performed using Fugene-6 transfection reagent (Roche) according to the manufacturer's protocol. At 2 days later, retroviral supernatants (10 ml) were collected serially during the subsequent 48 hr at 12 hr

(B and C) Abundance of methylated CpG dinucleotides as determined by bisulfite sequencing in the indicated subtelomeric regions. n = 17–55 clones were analyzed from a total of two cultures per cell type. Yellow and blue represent the frequency of methylated and unmethylated CpG dinucleotides, respectively. Gray corresponds to undetermined methylation. CpG, CpG position; U, unmethylated; M, methylated; n.p., not present. Chi-square test was used for statistical analysis, and the significant differences are indicated. Error bars, SD. MEF passage number = 2; iPS passage number = 8.

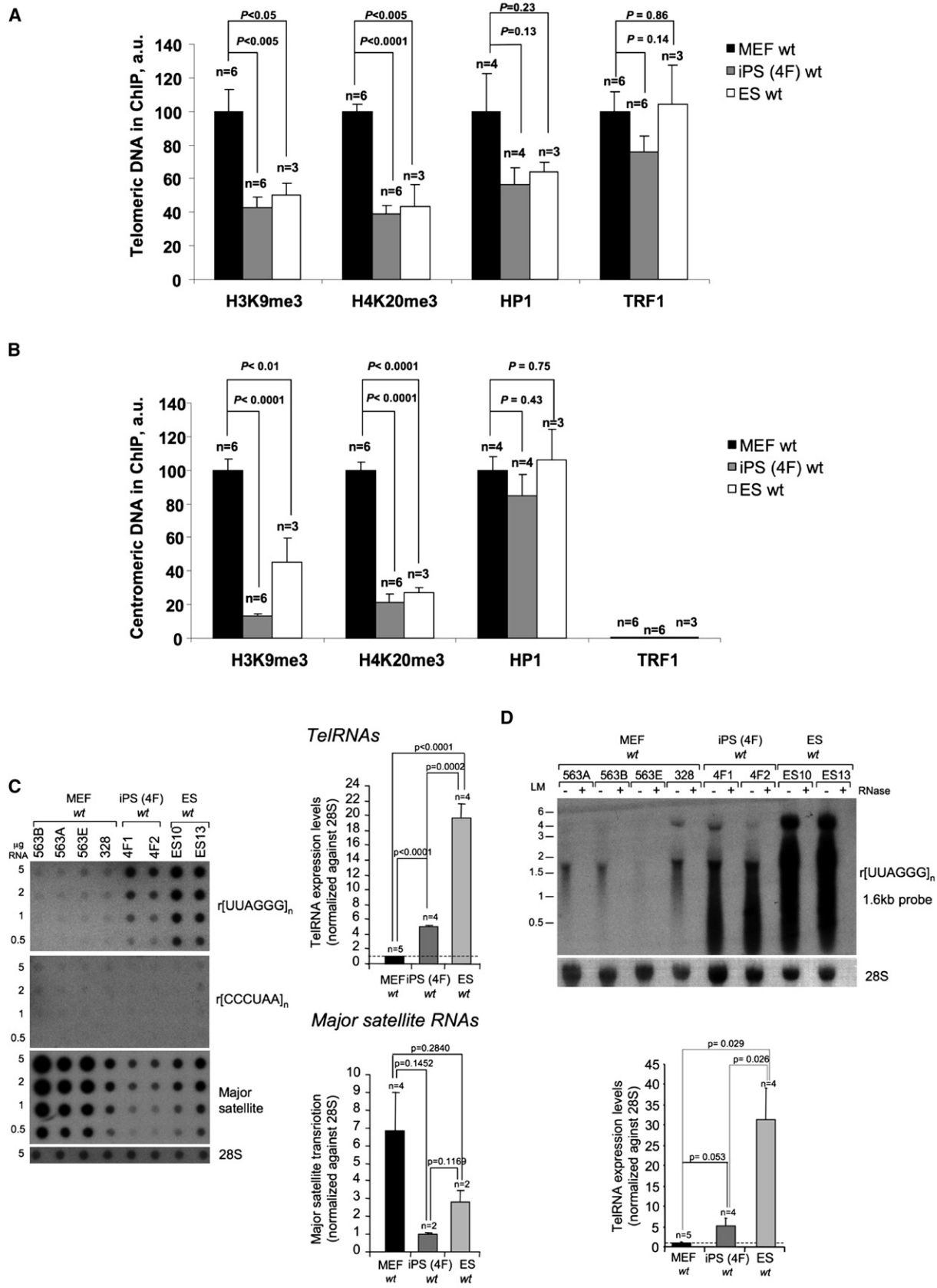
A
Telomeric DNA in ChIP, a.u.
H3K9me3
H4K20me3
HP1
TRF1
MEF wt
iPS (4F) wt
ES wt
B
Centromeric DNA in ChIP, a.u.
C
MEF wt
iPS (4F) wt
ES wt
563B
563A
563E
328
4F1
4F2
ES10
ES13
r[UUAGGG]n
r[CCCUAA]n
Major satellite
28S
TelRNAs
TelRNA expression levels (normalized against 28S)
Major satellite RNAs
Major satellite transriotion (normalized against 28S)
D
LM
RNase
r[UUAGGG]n
1.6kb probe
28S
TelRNA expression levels (normalized against 28S)

intervals, each time adding fresh medium to the cells (10 ml). The recipient MEF had been seeded the previous day (1–3 × 10^5 cells per 60 mm diameter dish) and received 1 ml of each of the corresponding retroviral supernatants (either a total of three or four). This procedure was repeated every 12 hr for 2 days (a total of four additions). After infection was completed, media was replaced with standard ES media supplemented with knockout serum replacement (KSR, Invitrogen). Cultures were maintained in the absence of drug selection (Blelloch et al., 2007) with daily medium changes. As early as 10 days after, colonies with ES-like morphology became visible at the microscope. Colonies were picked after 2–3 weeks and were expanded on feeder fibroblasts using standard procedures. For quantification of iPS generation efficiency, retroviral transduction was measured in parallel infections with three or four factors, as it applies, plus a GFP retroviral plasmid, followed by FACS analysis 2 days after infection was completed. The total number of iPS colonies was counted after staining plates for alkaline phosphatase activity (AP detection kit, Chemicon International) following the manufacturer's instruction.

The capacity of the iPS clones to generate chimeras in vivo was tested by microinjection into C57BL/6J-$Tyr^{(C-2J)/J}$ (albino) blastocysts (see Figure S1D) or by aggregation with CD1 (albino) morulae following standard procedures. So far, three independent wild-type iPS clones have been tested, two of them obtained by expression of four factors and one by expression of three factors. In all three cases, around 30% of the pups born were chimeras as judged by the coat color, with iPS contribution to the coat in a range of 60%–100% in the case of microinjected blastocysts and 30%–50% in the case of aggregation to morulae.

TRF Analysis

Cells were included in agarose plugs, and TRF analysis was performed as described previously (Blasco et al., 1997).

Q-FISH Analysis

We prepared metaphases and performed Q-FISH hybridization as previously described (Samper et al., 2001; Gonzalo et al., 2006). TFL-Telo software (Zijlmans et al., 1997) was used to quantify the fluorescence intensity of telomeres from at least five to ten metaphases for each data point.

Q-FISH comparing in vivo telomere length of iPS-derived mice was performed in tail skin sections as described (Muñoz et al., 2005). The telomere length in epidermal cells from iPS cell-derived chimeric mice was compared to that from tail skin derived from age-matched, sex-matched C57BL/6 controls obtained by standard breeding procedures. Telomere fluorescence intensity in 37 nuclei from each mouse was analyzed using the TFL-Telo software. Statistical analysis was performed using unpaired Student's t test comparing average fluorescence intensity in each mouse.

B1-SINE Cobra Analysis for Global DNA Methylation

Global DNA methylation levels were determined using the B1-SINE Cobra method as previously described (Benetti et al., 2007). Estimation of the fraction of methylated B1 elements for each genotype was done using the formula:

((molarity of 45 bp band) / 2)/((molarity of 45 bp band) + (molarity of 100 bp band)).

Analysis of Genomic Subtelomeric DNA Methylation

DNA methylation of subtelomeric genomic regions of the chromosome 1 and chromosome 2 (q arms) was established by PCR analysis after bisulfite modification as described (Benetti et al., 2007).

ChIP Assay

ChIP assays were performed as previously described (García-Cao et al., 2004) with the following antibodies: 6 ug of anti-histone H3 (# ab1791, Abcam), 6 μg of anti-histone H4 (# ab10158, Abcam), 6 μg of anti-H3K9me3 (#07-442, Upstate Biotechnology), 6 μg of anti-H4K20me3 (# 07-749, Upstate Biotechnology), 8 μl of rabbit polyclonal antibody to TRF1 (raised in our laboratory against full-length mouse TRF1 protein), 10 μl of monoclonal anti-HP-1γ (# 05-690, Upstate Biotechnology), or preimmune serum. The amount of telomeric and pericentric DNA after ChIP was normalized to the total telomeric or centromeric DNA signal, respectively, for each genotype, as well as to the H3 and H4 abundance at these domains, thus correcting for differences in the number of telomere repeats.

Telomere Transcription

Abundance of telomeric as centromeric transcripts was determined as previously described (Schoeftner and Blasco, 2008).

SUPPLEMENTAL DATA

The Supplemental Data include Supplemental Experimental Procedures and five figures and can be found with this article online at http://www.cell.com/cell-stem-cell/supplemental/S1934-5909(09)00002-2.

ACKNOWLEDGMENTS

M.A.B.'s laboratory is funded by the Spanish Ministry of Innovation and Science, the Consolider-Ingenio 2010 Program, the European Union, the Korber European Science Award, and the Spanish Association Against Cancer (AECC). K.S. is funded by the AECC.

Received: September 11, 2008
Revised: November 11, 2008
Accepted: December 30, 2008
Published: February 5, 2009

REFERENCES

Allsopp, R.C., Morin, G.B., DePinho, R., Harley, C.B., and Weissman, I.L. (2003). Telomerase is required to slow telomere shortening and extend replicative lifespan of HSCs during serial transplantation. Blood *102*, 517–520.

Aoi, T., Yae, K., Nakagawa, M., Ichisaka, T., Okita, K., Takahashi, K., Chiba, T., and Yamanaka, S. (2008). Generation of pluripotent stem cells from adult mouse liver and stomach cells. Science *321*, 699–702.

Armanios, M.Y., Chen, J.J., Cogan, J.D., Alder, J.K., Ingersoll, R.G., Markin, C., Lawson, W.E., Xie, M., Vulto, I., Phillips, J.A., III., et al. (2007). Telomerase mutations in families with idiopathic pulmonary fibrosis. N. Engl. J. Med. *356*, 1317–1326.

Azzalin, C.M., Reichenbach, P., Khoriauli, L., Giulotto, E., and Lingner, J. (2007). Telomeric repeat containing RNA and RNA surveillance factors at mammalian chromosome ends. Science *318*, 798–801.

Benetti, R., Gonzalo, S., Jaco, I., Schotta, G., Klatt, P., Jenuwein, T., and Blasco, M.A. (2007). Suv4-20h deficiency results in telomere elongation and derepression of telomere recombination. J. Cell Biol. *178*, 925–936.

Blackburn, E.H. (2001). Switching and signaling at the telomere. Cell *106*, 661–673.

Figure 4. Telomere Chromatin in Mouse iPS Cells Acquires the Features of ES Cell Telomeres

(A and B) Quantification of immunoprecipitated telomeric (A) and pericentric (B) repeats. Values were obtained after normalization to both DNA input signals and to abundance of H3 and H4 histones. Error bars correspond to three to six independent cell cultures (n) and refer to SE. Statistical analysis was performed using a Student's t test. MEF passage number = 2; iPS passage number = 8.

(C) Quantification of TelRNA and major satellite RNA levels by northern dot blot. Values were normalized against the signal for the 28S ribosomal subunit. Mean and standard error are shown. The number of individual values included in the statistical analysis is indicated (n).

(D) Northern of the indicated cell types shows increased TelRNAs levels in iPS cells. A probe for the 28S ribosomal subunit was used as a loading control. Numbers refer to independent cell cultures. Mean and standard error are shown. An unpaired t test was used to determine statistical significance. The number of independent cell lines analyzed is indicated (n). MEF passage number = 2; iPS passage number = 8.

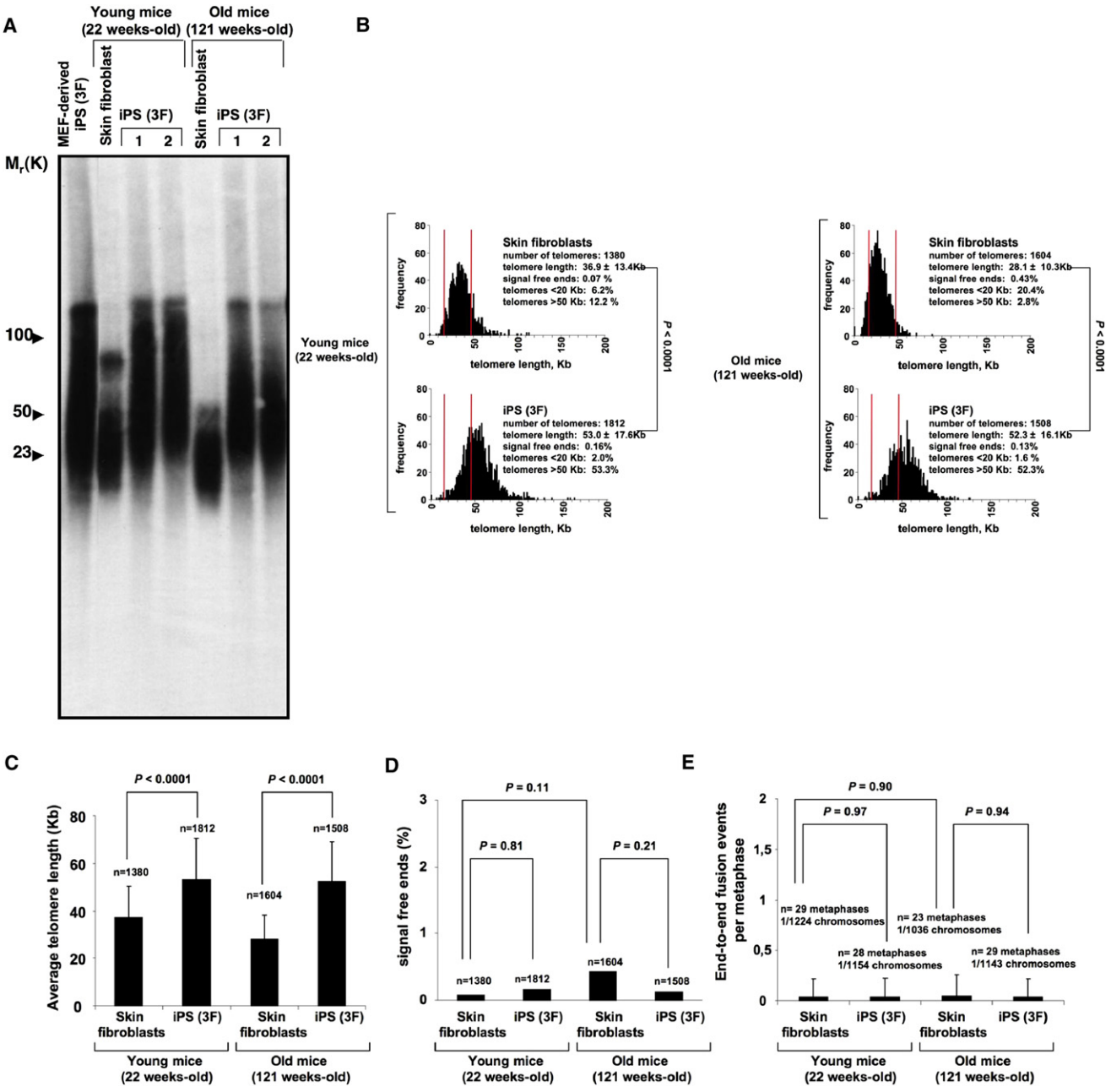

Figure 5. Telomere Elongation in Mouse iPS Cells Generated from Dermal Skin Fibroblasts of Young and Old Animals

(A) Telomere length by TRF analysis in mouse iPS cells derived from differentiated skin fibroblasts of young (22 weeks old) or old (121 weeks old) mice. Fibroblast passage number = 2; iPS passage number = 8. Numbers refer to independent cell cultures.

(B) Telomere length distributions by metaphase Q-FISH in mouse iPS cells derived from differentiated skin fibroblasts of young (22 weeks old) or old (121 weeks old) mice. Fibroblast passage number = 2; iPS passage number = 8. A Wilcoxon-Mann-Whitney rank sum test was used to calculate statistical significance of the observed differences in the mean telomere length.

(C) Quantification of average telomere length in kilobases in the indicated cells. n, number of telomeres. Error bars, SD. Fibroblast passage number = 2; iPS passage number = 8.

(D) Quantification of the percentage of signal-free ends in the indicated cells. Fibroblast passage number = 2; iPS passage number = 8. Statistical comparisons using the chi-square test are shown.

(E) Frequency of end-to-end chromosome fusions in metaphase spreads from mouse iPS cells derived from differentiated skin fibroblasts of young or old mice. Number of metaphases used for the analysis as well as number of fusion events detected are indicated. Fibroblast passage number = 2; iPS passage number = 8. Chi-square test was used for statistical analysis. Error bars, SD.

Blasco, M.A. (2005). Telomeres and human disease: Ageing, cancer and beyond. Nat. Rev. Genet. *6*, 611–622.

Blasco, M.A. (2007a). Telomere length, stem cells and aging. Nat. Chem. Biol. *3*, 640–649.

Blasco, M.A. (2007b). The epigenetic regulation of mammalian telomeres. Nat. Rev. Genet. *8*, 299–309.

Blasco, M.A., Lee, H.W., Hande, M.P., Samper, E., Lansdorp, P.M., DePinho, R.A., and Greider, C.W. (1997). Telomere shortening and tumor formation by mouse cells lacking telomerase RNA. Cell *91*, 25–34.

Blelloch, R., Venere, M., Yen, J., and Ramalho-Santos, M. (2007). Generation of induced pluripotent stem cells in the absence of drug selection. Cell Stem Cell *1*, 245–247.

de Lange, T. (2005). Shelterin: The protein complex that shapes and safeguards human telomeres. Genes Dev. *19*, 2100–2110.

de Lange, T., Shiue, L., Myers, R.M., Cox, D.R., Naylor, S.L., Killery, A.M., and Varmus, H.E. (1990). Structure and variability of human chromosome ends. Mol. Cell. Biol. *10*, 518–527.

Dimos, J.T., Rodolfa, K.T., Niakan, K.K., Weisenthal, L.M., Mitsumoto, H., Chung, W., Croft, G.F., Saphier, G., Leibel, R., Goland, R., et al. (2008). Induced pluripotent stem cells generated from patients with ALS can be differentiated into motor neurons. Science *321*, 1218–1221.

Dunham, M.A., Neumann, A.A., Fasching, C.L., and Reddel, R.R. (2000). Telomere maintenance by recombination in human cells. Nat. Genet. *26*, 447–450.

Ferrón, S., Mira, H., Franco, S., Cano-Jaimez, M., Bellmunt, E., Ramírez, C., Fariñas, I., and Blasco, M.A. (2004). Telomere shortening and chromosomal instability abrogates proliferation of adult but not embryonic neural stem cells. Development *131*, 4059–4070.

Flores, I., Cayuela, M.L., and Blasco, M.A. (2005). Effects of telomerase and telomere length on epidermal stem cell behavior. Science *309*, 1253–1256.

Flores, I., Benetti, R., and Blasco, M.A. (2006a). Telomerase regulation and stem cell behaviour. Curr. Opin. Cell Biol. *18*, 254–260.

Flores, I., Evan, G., and Blasco, M.A. (2006b). Genetic analysis of myc and telomerase interactions in vivo. Mol. Cell. Biol. *26*, 6130–6138.

Flores, I., Canela, A., Vera, E., Tejera, A., Cotsarelis, G., and Blasco, M.A. (2008). The longest telomeres: A general signature of adult stem cell compartments. Genes Dev. *22*, 654–667.

García-Cao, M., O'Sullivan, R., Peters, A.H., Jenuwein, T., and Blasco, M.A. (2004). Epigenetic regulation of telomere length in mammalian cells by the Suv39h1 and Suv39h2 histone methyltransferases. Nat. Genet. *36*, 94–99.

Gonzalo, S., Jaco, I., Fraga, M.F., Chen, T., Li, E., Esteller, M., and Blasco, M.A. (2006). DNA methyltransferases control telomere length and telomere recombination in mammalian cells. Nat. Cell Biol. *8*, 416–424.

Greider, C.W., and Blackburn, E.H. (1985). Identification of a specific telomere terminal transferase activity in Tetrahymena extracts. Cell *43*, 405–413.

Harley, C.B., Futcher, A.B., and Greider, C.W. (1990). Telomeres shorten during ageing of human fibroblasts. Nature *345*, 458–460.

Hemann, M.T., Strong, M.A., Hao, L.Y., and Greider, C.W. (2001). The shortest telomere, not average telomere length, is critical for cell viability and chromosome stability. Cell *107*, 67–77.

Herrera, E., Samper, E., Martín-Caballero, J., Flores, J.M., Lee, H.W., and Blasco, M.A. (1999). Disease states associated with telomerase deficiency appear earlier in mice with short telomeres. EMBO J. *18*, 2950–2960.

Lanza, R.P., Cibelli, J.B., Blackwell, C., Cristofalo, V.J., Francis, M.K., Baerlocher, G.M., Mak, J., Schertzer, M., Chavez, E.A., Sawyer, N., et al. (2000). Extension of cell life-span and telomere length in animals cloned from senescent somatic cells. Science *288*, 665–669.

Lee, H.W., Blasco, M.A., Gottlieb, G.J., Horner, J.W., II, Greider, C.W., and DePinho, R.A. (1998). Essential role of mouse telomerase in highly proliferative organs. Nature *392*, 569–574.

Liu, L., Bailey, S.M., Okuka, M., Muñoz, P., Li, C., Zhou, L., Wu, C., Czerwiec, E., Sandler, L., Seyfang, A., et al. (2007). Telomere lengthening early in development. Nat. Cell Biol. *9*, 1436–1441.

Maherali, N., Sridharan, R., Xie, W., Utikal, J., Eminli, S., Arnold, K., Stadtfeld, M., Yachechko, R., Tchieu, J., Jaenisch, R., et al. (2007). Directly reprogrammed fibroblasts show global epigenetic remodeling and widespread tissue contribution. Cell Stem Cell *1*, 55–70.

Meeker, A.K., Hicks, J.L., Gabrielson, E., Strauss, W.M., De Marzo, A.M., and Argani, P. (2004). Telomere shortening occurs in subsets of normal breast epithelium as well as in situ and invasive carcinoma. Am. J. Pathol. *164*, 925–935.

Meshorer, E., Yellajoshula, D., George, E., Scambler, P.J., Brown, D.T., and Misteli, T. (2006). Hyperdynamic plasticity of chromatin proteins in pluripotent embryonic stem cells. Dev. Cell *10*, 105–116.

Mikkelsen, T.S., Hanna, J., Zhang, X., Ku, M., Wernig, M., Schorderet, P., Bernstein, B.E., Jaenisch, R., Lander, E.S., and Meissner, A. (2008). Dissecting direct reprogramming through integrative genomic analysis. Nature *454*, 49–55.

Mitchell, J.R., Wood, E., and Collins, K. (1999). A telomerase component is defective in the human disease dyskeratosis congenita. Nature *402*, 551–555.

Muñoz, P., Blanco, R., Flores, J.M., and Blasco, M.A. (2005). XPF nuclease dependent telomere loss and increased DNA damage in mice overexpressing TRF2 result in premature aging and cancer. Nat. Genet. *10*, 1063–1071.

Nakagawa, M., Koyanagi, M., Tanabe, K., Takahashi, K., Ichisaka, T., Aoi, T., Okita, K., Mochiduki, Y., Takizawa, N., and Yamanaka, S. (2008). Generation of induced pluripotent stem cells without Myc from mouse and human fibroblasts. Nat. Biotechnol. *26*, 101–106.

Okita, K., Ichisaka, T., and Yamanaka, S. (2007). Generation of germline-competent induced pluripotent stem cells. Nature *448*, 313–317.

Samper, E., Flores, J.M., and Blasco, M.A. (2001). Restoration of telomerase activity rescues chromosomal instability and premature aging in Terc−/− mice with short telomeres. EMBO Rep. *2*, 800–807.

Samper, E., Fernández, P., Eguía, R., Martín-Rivera, L., Bernad, A., Blasco, M.A., and Aracil, M. (2002). Long-term repopulating ability of telomerase-deficient murine hematopoietic stem cells. Blood *99*, 2767–2775.

Schoeftner, S., and Blasco, M.A. (2008). Developmentally regulated transcription of mammalian telomeres by DNA-dependent RNA polymerase II. Nat. Cell Biol. *10*, 228–236.

Shiels, P.G., Kind, A.J., Campbell, K.H., Wilmut, I., Waddington, D., Colman, A., and Schnieke, A.E. (1999). Analysis of telomere lengths in cloned sheep. Nature *399*, 316–317.

Siegl-Cachedenier, I., Flores, I., Klatt, P., and Blasco, M.A. (2007). Telomerase reverses epidermal hair follicle stem cell defects and loss of long-term survival associated with critically short telomeres. J. Cell Biol. *179*, 277–290.

Stadtfeld, M., Maherali, N., Breault, D.T., and Hochedlinger, K. (2008). Defining molecular cornerstones during fibroblast to iPS cell reprogramming in mouse. Cell Stem Cell *2*, 230–240.

Takahashi, K., and Yamanaka, S. (2006). Induction of pluripotent stem cells from mouse embryonic and adult fibroblast cultures by defined factors. Cell *126*, 663–676.

Takahashi, K., Tanabe, K., Ohnuki, M., Narita, M., Ichisaka, T., Tomoda, K., and Yamanaka, S. (2007). Induction of pluripotent stem cells from adult human fibroblasts by defined factors. Cell *131*, 861–872.

Tsakiri, K.D., Cronkhite, J.T., Kuan, P.J., Xing, C., Raghu, G., Weissler, J.C., Rosenblatt, R.L., Shay, J.W., and Garcia, C.K. (2007). Adult-onset pulmonary fibrosis caused by mutations in telomerase. Proc. Natl. Acad. Sci. USA *104*, 7552–7557.

Vogel, G. (2000). In contrast to Dolly, cloning resets telomere clock in cattle. Science *288*, 586–587.

Wakayama, T., Shinkai, Y., Tamashiro, K.L., Niida, H., Blanchard, D.C., Blanchard, R.J., Ogura, A., Tanemura, K., Tachibana, M., Perry, A.C., et al. (2000). Cloning of mice to six generations. Nature *407*, 318–319.

Wernig, M., Meissner, A., Foreman, R., Brambrink, T., Ku, M., Hochedlinger, K., Bernstein, B.E., and Jaenisch, R. (2007). *In vitro* reprogramming of fibroblasts into a pluripotent ES-cell-like state. Nature *448*, 318–324.

Wernig, M., Meissner, A., Cassady, J.P., and Jaenisch, R. (2008). c-Myc is dispensable for direct reprogramming of mouse fibroblasts. Cell Stem Cell *2*, 10–12.

Wu, K.J., Grandori, C., Amacker, M., Simon-Vermot, N., Polack, A., Lingner, J., and Dalla-Favera, R. (1999). Direct activation of TERT transcription by c-MYC. Nat. Genet. *21*, 220–224.

Yamaguchi, H., Calado, R.T., Ly, H., Kajigaya, S., Baerlocher, G.M., Chanock, S.J., Lansdorp, P.M., and Young, N.S. (2005). Mutations in TERT, the gene for telomerase reverse transcriptase, in aplastic anemia. N. Engl. J. Med. *352*, 1413–1424.

Zhao, R., and Daley, G.Q. (2008). From fibroblasts to iPS cells: Induced pluripotency by defined factors. J. Cell. Biochem. *105*, 949–955.

Zijlmans, J.M., Martens, U.M., Poon, S.S., Raap, A.K., Tanke, H.J., Ward, R.K., and Lansdorp, P.M. (1997). Telomeres in the mouse have large inter-chromosomal variations in the number of T2AG3 repeats. Proc. Natl. Acad. Sci. USA *94*, 7423–7428.